

***Caenorhabditis elegans* *brc-1* mutation increases the number of COSA-1 foci in *him-8* and *zim-2* mutants**

Takamune T. Saito^{1,2§}, Koki Yamamoto^{1,3}, Hirohito Minami², Taiki Tsujiue¹

¹Department of Genetic Engineering, Faculty of Biology-Oriented Science and Technology, Kindai University, Kinokawa, Wakayama, Japan

²Graduate School of Biology-Oriented Science and Technology, Kindai University, Kinokawa, Wakayama, Japan

³Present address: Graduate School of Biostudies, Kyoto University, Kyoto, Japan

[§]To whom correspondence should be addressed: tsaito@waka.kindai.ac.jp

Abstract

Crossover designation factors such as [COSA-1](#) are concentrated at the specific DNA double-strand break (DSB) sites to promote crossover formation. [zim-1](#) mutants, which show defects in the homologous chromosome pairing of chromosomes II and III, increase the [COSA-1](#) foci/normal bivalent state compared to the expected value. The excess designation was suppressed by an additional mutation in [brc-1](#) in [zim-1](#) mutants. We demonstrated that the number of [COSA-1](#) foci in [him-8](#) and [zim-2](#) mutants, showing defects in the pairing of the X and V chromosomes, respectively, increased compared to the expected value, and [brc-1](#) mutation accelerated the number of [COSA-1](#) foci in oogenesis.

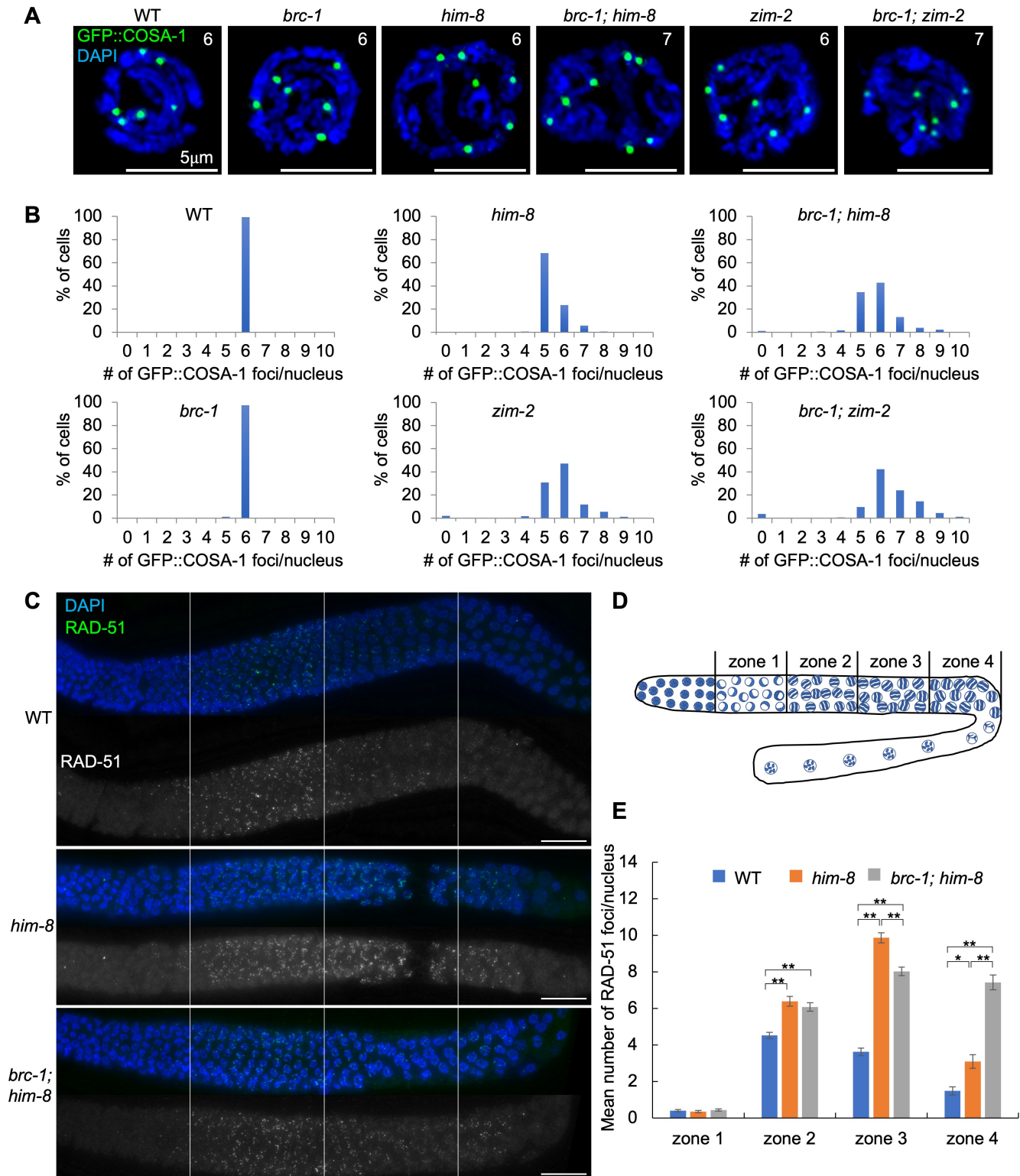


Figure 1. Deletion of BRC-1 increases the number of COSA-1 and RAD-51 foci at late pachytene in *him-8* and *zim-2* mutants:

(A) Representative images of GFP::COSA-1 in indicated strains. The numbers in the panels indicate the number of GFP::COSA-1 foci. Scale bars, 5 μ m. (B) Graphs showing the quantification of GFP::COSA-1 foci/nucleus in the late pachytene stage in each strain. N-value, WT = 6 gonads, 256 cells; *brc-1* mutants = 10 gonads, 267 cells; *him-8* mutants = 10 gonads, 272 cells; *brc-1; him-8* double mutants = 9 gonads, 182 cells; *zim-2* mutants = 18 gonads, 295 cells, *brc-1; zim-2*

double mutants = 18 gonads, 326 cells. (C) Representative images of RAD-51 immunostaining in the gonads. Perpendicular white lines indicate the border of each zone. Scale bars, 20 μm . (D) Illustration of the gonad divided into four zones of equal length from the transition zone to late pachytene (zone 1, transition zone; zone 2, early pachytene; zone 3, mid-pachytene; and zone 4, late pachytene). (E) Graphs showing the average number of RAD-51 foci per nucleus in different zones. Error bars represent the standard error of the mean. Asterisks indicate statistical difference (* $p=0.01732$, ** $p<0.00001$, two-tailed Mann-Whitney test). N-value, WT = 3 gonads, 250, 235, 138, and 90 cells per zone. [him-8](#) mutants = 3 gonads, 177, 206, 147, and 97 cells per zone. [brc-1](#); [him-8](#) mutants = 4 gonads, 264, 224, 167, and 96 cells per zone.

Description

Meiosis is a cell division process that generates haploid gametes from diploid parental cells. Crossover formation is essential for appropriate homologous chromosome segregation of meiosis I. A single crossover event per homologous chromosome pair is observed in wild-type *Caenorhabditis elegans*. The process of selecting a specific DNA double-strand break (DSB) as a future crossover site is called crossover designation (Kleckner *et al.* 2003; Gray and Cohen 2016). Crossover designation factors such as [COSA-1](#), [MSH-5](#), and [ZHP-3](#) concentrate at the sites of DSBs, which are further repaired by crossover (Kelly *et al.* 2000; Jantsch *et al.* 2004; Bhalla *et al.* 2008; Yokoo *et al.* 2012). Therefore, six [COSA-1](#) foci are observed in the nucleus at the late pachytene stage in the wild-type (Yokoo *et al.* 2012).

Homologous chromosomes begin to pair at the pairing center via pairing center-binding proteins ([ZIM-1](#), [ZIM-2](#), [ZIM-3](#), and [HIM-8](#)) during the leptotene-zygotene transition (Phillips *et al.* 2005; Phillips and Dernburg 2006). The homologous pairing of chromosomes II and III is impaired in [zim-1](#) mutants (Phillips and Dernburg 2006). Although [zim-1](#) mutants are expected to have four [COSA-1](#) foci per nucleus, an average of 6.12 [COSA-1](#) foci are observed in these mutants (Li *et al.* 2018). The mutation of [brc-1](#), which is a homolog of human breast cancer gene 1 (BRCA1) (Futreal *et al.* 1994; Miki *et al.* 1994; Boulton *et al.* 2004), suppresses the increase in GFP::[COSA-1](#) foci in [brc-1](#); [zim-1](#) double mutants (4.3–4.8 [COSA-1](#) foci/nucleus) (Li *et al.* 2018). In this study, we investigated whether [him-8](#) and [zim-2](#) mutants, in which the pairing of the X and V chromosomes, respectively, is defective (Phillips *et al.* 2005; Phillips and Dernburg 2006), show an increase in [COSA-1](#) foci compared to the expected value (5 foci/nucleus), and whether the phenotypes were suppressed by the [brc-1](#) mutation.

We quantified the GFP::[COSA-1](#) foci in the late pachytene stage in the wild-type, [him-8](#), [brc-1](#), [zim-2](#) single mutants, and [brc-1](#); [him-8](#), [brc-1](#); [zim-2](#) double mutants by 3D-fluorescent microscopy. As previously shown by many groups, six GFP::[COSA-1](#) foci were observed in the wild-type (Figure 1A, 1B). If a single crossover event was hypothesized to occur per homologous chromosome pair, then we would expect to observe five GFP::[COSA-1](#) foci/nucleus in [him-8](#) mutants with unpaired X chromosomes and in [zim-2](#) mutants with unpaired chromosome V. However, in addition to five foci of GFP::[COSA-1](#)/nucleus, we observed that 30.5% and 65.4% of cells had more than six foci of GFP::[COSA-1](#) in [him-8](#) and [zim-2](#) mutants, respectively (Figure 1A, 1B). This phenotype was similar to that observed in [zim-1](#) mutants (Li *et al.* 2018). These data suggest that the interchromosomal effect causes excess crossover in a normal pair of homologous chromosomes if crossover formation does not occur in one or two sets of unpaired chromosomes during *C. elegans* oocyte meiosis (Herman and Kari 1989; Carlton *et al.* 2006; Li *et al.* 2018). A similar increase in crossover formation between normal chromosome pairs has been observed during *Drosophila* female meiosis when chromosomal rearrangements (heterozygous inversions or translocations) are present in the cell (Sturtevant 1919; Sturtevant 1921).

Furthermore, we examined whether the [brc-1](#) mutation suppressed the number of [COSA-1](#) foci in a [him-8](#) and [zim-2](#) backgrounds. Similar to the wild-type, 97.4% of cells showed six GFP::[COSA-1](#) foci in [brc-1](#) mutants (Figure 1A, 1B). GFP::[COSA-1](#) foci were further increased in [brc-1](#); [him-8](#) and [brc-1](#); [zim-2](#) double mutants compared to [him-8](#) and [zim-2](#) single mutants. A total of 62.1% and 86.5% of cells had more than six foci of GFP::[COSA-1](#) in [brc-1](#); [him-8](#) and [brc-1](#); [zim-2](#) double mutants, respectively ($p<0.00001$; Mann-Whitney U test, comparison with each single mutant). These results suggest that [BRC-1](#) suppresses the excess of [COSA-1](#) foci in the [him-8](#) and [zim-2](#) mutant backgrounds.

One of the major roles of [BRC-1](#) is to stabilize RAD-51 filaments when crossover formation is impaired (Janisiw *et al.* 2018; Li *et al.* 2018). RAD-51 levels in pachytene are elevated in [him-8](#) and [zim-1](#) mutants compared to those in the wild-type (Carlton *et al.* 2006; Li *et al.* 2018). Removal of [BRC-1](#) in [zim-1](#) mutants results in a “dark zone” of RAD-51 in mid to late pachytene in which the accumulation of RAD-51 foci are suppressed (Li *et al.* 2018). To examine whether [BRC-1](#) promotes RAD-51 filament stability in [him-8](#) mutants, we compared RAD-51 levels in four individual zones from the first cell of the transition zone to the end of late pachytene in the wild-type, [him-8](#), and [brc-1](#); [him-8](#) double mutants (Figure 1C, 1D, 1E). Similar to a previous study, the levels of RAD-51 foci were elevated in all pachytene stages (zones 2, 3, and 4) in [him-8](#) mutants compared with the wild-type (Carlton *et al.* 2006) (Figure 1C, 1E). The RAD-51 levels were decreased to 81% in mid-pachytene (zone 3) in [brc-1](#); [him-8](#) double mutants compared to [him-8](#) single mutants ($p<0.0001$); however, obvious RAD-51 dark zone was not observed in [brc-1](#); [him-8](#) double mutants. Most RAD-51 foci remain in the late pachytene stage

(zone 4) in [brc-1; him-8](#) double mutants compared with [him-8](#) single mutants ($p < 0.0001$). These results suggest that the contribution of [BRC-1](#) to RAD-51 filament stability at mid-pachytene in [him-8](#) mutants was not as high as that in the [zim-1](#) mutant.

We observed an excess number of GFP::COSA-1 foci in the [him-8](#) and [zim-2](#) single mutants compared with the expected value of the five autosome pairs. These findings are consistent with those of previous studies, which demonstrated that crossover formation increases in autosomes during oogenesis in [him-8](#) mutants (Herman and Kari 1989; Carlton *et al.* 2006). These data suggest that interchromosomal effects occur in [him-8](#) and [zim-2](#) mutants, similar to [zim-1](#) mutants (Li *et al.* 2018).

The phenotypes of [brc-1; him-8 \(zim-2\)](#) and [brc-1; zim-1](#) differed during oogenesis. The [brc-1](#) mutation suppresses the formation of [COSA-1](#) foci in [zim-1](#) mutants (Li *et al.* 2018), whereas the [brc-1](#) mutation enhanced the formation of [COSA-1](#) foci in [him-8](#) and [zim-2](#) mutants in the present study. A RAD-51 dark zone was observed in [brc-1; zim-1](#) double mutants (Li *et al.* 2018), whereas in [brc-1; him-8](#) double mutants, a slight decrease in RAD-51 levels, but no clear RAD-51 dark zone, was observed. These observations suggest that the function of [BRC-1](#) in the formation of [COSA-1](#) foci and the processing (removal/stabilization) of RAD-51 may be regulated differently according to the number of chromosome pairs involved in oogenesis. Furthermore, [COSA-1](#) foci formation is differentially regulated during oogenesis and male spermatogenesis (Li *et al.* 2020). The single X chromosome condition in wild-type, [him-8](#) mutant, and [brc-1; him-8](#) double mutant males did not increase the number of [COSA-1](#) foci compared with the hypothesized number of five [COSA-1](#) foci (Li *et al.* 2020). In contrast to oogenesis, [brc-1; zim-1](#) males demonstrated enhanced formation of [COSA-1](#) foci compared to [zim-1](#) single mutants (Li *et al.* 2020). Further research is required to explore the sex-specific regulation of crossover designs under pairing defect conditions.

Methods

Fixation and immunostaining:

Worms expressing GFP::COSA-1 (post L4 22–24 h) were dissected using a scalpel. For dissection, 30 μ L of 15 mM sodium azide solution was placed on a cover glass, followed by approximately 20 worms. After removing 15 μ L of the sodium azide solution, 15 μ L of 2% Paraformaldehyde (PFA) was added, mixed to a final concentration of 1% PFA and left for 5 min to fix. After removing 15 μ L of the mixture, the sample was sandwiched in a slide glass. The slide was placed at -80°C for 5 min. After removing the cover glass by cracking it with a razor blade, it was fixed again in ice-cold methanol (-20°C) for 1 min. Immunostaining was performed as previously described (Saito *et al.* 2009). The primary and secondary antibodies used in this study were rabbit anti-RAD-51 antibody (Das *et al.* 2022), 1:3,000 and goat FITC-conjugated anti-rabbit antibody (Jackson ImmunoResearch, 1:200), respectively. The sample was then washed with phosphate-buffered saline with Tween 20 for 5 min for three times, mounted with 8 μ L VECTASHIELD with 4',6-diamidino-2-phenylindole (Vector laboratories, Burlingame, California, USA), and the cover glass was shielded by nail polish.

Imaging:

Images were obtained using an all-in-one fluorescence microscope (BZ-X800; KEYENCE, Osaka, Japan) equipped with a Plan Achromat 100x objective (NA1.45; BZ-PA100; KEYENCE). Approximately 30–40 Z-stack images of germline nuclei were captured at intervals of 0.2 μ m. Green fluorescence was detected using a GFP filter (excitation, 470/40 nm; emission, 525/50 nm; dichroism, 495 nm; OP-87763; KEYENCE, Osaka, Japan). The BZ-X analysis software (BZ-H4A) and a 3D application (BZ-H4R) were used for the analysis.

Reagents

Strains:

Strain	Genotype	Available from
N2	<i>Caenorhabditis elegans</i> wild-type	CGC
TTS65	brc-1(tm1145) III	NBRP
TTS185	him-8(tm611) IV	NBRP
TTS272	zim-2(tm574) IV	NBRP, CGC

TTS186	brc-1(tm1145) III; him-8(tm611) IV	Saito lab
TTS321	brc-1(tm1145) III; zim-2(tm574) IV	Saito lab
AV630	meIs8[pie-1promoter::gfp::cosa-1 + unc-119(+)] II	Villeneuve lab, CGC
TTS171	meIs8[pie-1promoter::gfp::cosa-1 + unc-119(+)] II; brc-1(tm1145) III	Saito lab
TTS175	meIs8[pie-1promoter::gfp::cosa-1 + unc-119(+)] II; him-8(tm611) IV	Saito lab
TTS320	meIs8[pie-1promoter::gfp::cosa-1 + unc-119(+)] II; zim-2(tm574) IV	Saito lab
TTS174	meIs8[pie-1promoter::gfp::cosa-1 + unc-119(+)] II; brc-1(tm1145) III; him-8(tm611) IV	Saito lab
TTS319	meIs8[pie-1promoter::gfp::cosa-1 + unc-119(+)] II; brc-1(tm1145) III; zim-2(tm574) IV	Saito lab

After receiving the original strains, [TTS65](#), [TTS185](#), [TTS186](#), [TTS272](#), and [AV630](#) were outcrossed six times with [N2](#) at the Saito Laboratory.

Acknowledgements:

Some strains were kindly provided by the *Caenorhabditis* Genetics Center (CGC) funded by the NIH Office of Research Infrastructure Programs (P40 OD010440) and the National BioResource Project (NBRP) funded by the Japanese government. We thank Nicola Silva for providing the rabbit anti-RAD-51 antibody, JoAnne Engebrecht, Peter Carlton, Aya Sato and members of the Saito lab for helpful discussion on this work. Initial preparation of the strains was performed by Kae Akamatsu, Eno Honda, and Kaito Tanaka in the Saito laboratory. This work was supported by the Japan Society for the Promotion of Science (JSPS) KAKENHI Grants JP19K06784 and JP23K05868 to TTS.

References

- Bhalla N, Wynne DJ, Jantsch V, Dernburg AF. 2008. ZHP-3 acts at crossovers to couple meiotic recombination with synaptonemal complex disassembly and bivalent formation in *C. elegans*. *PLoS Genet* 4(10): e1000235. PubMed ID: [18949042](#)
- Boulton SJ, Martin JS, Polanowska J, Hill DE, Gartner A, Vidal M. 2004. BRCA1/BARD1 orthologs required for DNA repair in *Caenorhabditis elegans*. *Curr Biol* 14(1): 33-9. PubMed ID: [14711411](#)
- Carlton PM, Farruggio AP, Dernburg AF. 2006. A link between meiotic prophase progression and crossover control. *PLoS Genet* 2(2): e12. PubMed ID: [16462941](#)
- Futreal PA, Liu Q, Shattuck-Eidens D, Cochran C, Harshman K, Tavtigian S, et al., Miki Y. 1994. BRCA1 mutations in primary breast and ovarian carcinomas. *Science* 266(5182): 120-2. PubMed ID: [7939630](#)
- Jantsch V, Pasierbek P, Mueller MM, Schweizer D, Jantsch M, Loidl J. 2004. Targeted gene knockout reveals a role in meiotic recombination for ZHP-3, a Zip3-related protein in *Caenorhabditis elegans*. *Mol Cell Biol* 24(18): 7998-8006. PubMed ID: [15340062](#)
- Kelly KO, Dernburg AF, Stanfield GM, Villeneuve AM. 2000. *Caenorhabditis elegans* msh-5 is required for both normal and radiation-induced meiotic crossing over but not for completion of meiosis. *Genetics* 156(2): 617-30. PubMed ID: [11014811](#)
- Li Q, Saito TT, Martinez-Garcia M, Deshong AJ, Nadarajan S, Lawrence KS, et al., Engebrecht J. 2018. The tumor suppressor BRCA1-BARD1 complex localizes to the synaptonemal complex and regulates recombination under meiotic dysfunction in *Caenorhabditis elegans*. *PLoS Genet* 14(11): e1007701. PubMed ID: [30383767](#)
- Li Q, Hariri S, Engebrecht J. 2020. Meiotic Double-Strand Break Processing and Crossover Patterning Are Regulated in a Sex-Specific Manner by BRCA1-BARD1 in *Caenorhabditis elegans*. *Genetics* 216(2): 359-379. PubMed ID: [32796008](#)
- Miki Y, Swensen J, Shattuck-Eidens D, Futreal PA, Harshman K, Tavtigian S, et al., Ding W. 1994. A strong candidate for the breast and ovarian cancer susceptibility gene BRCA1. *Science* 266(5182): 66-71. PubMed ID: [7545954](#)

- Phillips CM, Dernburg AF. 2006. A family of zinc-finger proteins is required for chromosome-specific pairing and synapsis during meiosis in *C. elegans*. *Dev Cell* 11(6): 817-29. PubMed ID: [17141157](#)
- Phillips CM, Meng X, Zhang L, Chretien JH, Urnov FD, Dernburg AF. 2009. Identification of chromosome sequence motifs that mediate meiotic pairing and synapsis in *C. elegans*. *Nat Cell Biol* 11(8): 934-42. PubMed ID: [19620970](#)
- Sturtevant, A.H. 1919. Inherited linkage variations in the second chromosome. Contributions to the genetics of *Drosophila melanogaster*. III. Carnegie Institution, Washington 278:307–341.
- Sturtevant AH. 1921. A Case of Rearrangement of Genes in *Drosophila*. *Proc Natl Acad Sci U S A* 7(8): 235-7. PubMed ID: [16576597](#)
- Yokoo R, Zawadzki KA, Nabeshima K, Drake M, Arur S, Villeneuve AM. 2012. COSA-1 reveals robust homeostasis and separable licensing and reinforcement steps governing meiotic crossovers. *Cell* 149(1): 75-87. PubMed ID: [22464324](#)
- Das D, Trivedi S, Blazicková J, Arur S, Silva N. 2022. Phosphorylation of HORMA-domain protein HTP-3 at Serine 285 is dispensable for crossover formation. *G3 Genes|Genomes|Genetics* 12: 10.1093/g3journal/jkac079. PubMed ID: [9073698](#)
- Gray S, Cohen PE. 2016. Control of Meiotic Crossovers: From Double-Strand Break Formation to Designation. *Annual Review of Genetics* 50: 175-210. PubMed ID: [27648641](#)
- Herman RK, Kari CK. 1989. Recombination between small X chromosome duplications and the X chromosome in *Caenorhabditis elegans*. *Genetics* 121: 723-737. PubMed ID: [2721932](#)
- Janisiw E, Dello Stritto MR, Jantsch V, Silva N. 2018. BRCA1-BARD1 associate with the synaptonemal complex and pro-crossover factors and influence RAD-51 dynamics during *Caenorhabditis elegans* meiosis. *PLOS Genetics* 14: e1007653. PubMed ID: [30383754](#)
- Kleckner N, Storlazzi A, Zickler D. 2003. Coordinate variation in meiotic pachytene SC length and total crossover/chiasma frequency under conditions of constant DNA length. *Trends in Genetics* 19: 623-628. PubMed ID: [14585614](#)
- Saito TT, Youds JL, Boulton SJ, Colaiácovo MP. 2009. *Caenorhabditis elegans* HIM-18/SLX-4 Interacts with SLX-1 and XPF-1 and Maintains Genomic Integrity in the Germline by Processing Recombination Intermediates. *PLoS Genetics* 5: e1000735. PubMed ID: [19936019](#)

Funding:

Supported by Japan Society for the Promotion of Science (Japan) JP19K06784, JP23K05868 to TTS.

Author Contributions: Takamune T. Saito: conceptualization, data curation, formal analysis, funding acquisition, investigation, methodology, project administration, supervision, validation, visualization, writing - original draft, writing - review editing. Koki Yamamoto: investigation, validation. Hirohito Minami: investigation. Taiki Tsujiue: validation.

Reviewed By: Anonymous

Nomenclature Validated By: Anonymous

WormBase Paper ID: WBPaper00066950

History: Received December 2, 2023 **Revision Received** June 21, 2024 **Accepted** July 22, 2024 **Published Online** July 25, 2024 **Indexed** August 8, 2024

Copyright: © 2024 by the authors. This is an open-access article distributed under the terms of the Creative Commons Attribution 4.0 International (CC BY 4.0) License, which permits unrestricted use, distribution, and reproduction in any medium, provided the original author and source are credited.

Citation: Saito, TT; Yamamoto, K; Minami, H; Tsujiue, T (2024). *Caenorhabditis elegans* *brc-1* mutation increases the number of COSA-1 foci in *him-8* and *zim-2* mutants. *microPublication Biology*. [10.17912/micropub.biology.001077](https://doi.org/10.17912/micropub.biology.001077)